

S. Sivakumar, Ravikiran Sangras and Vasudevan Raghavan\*

# Effect of Grid Generated Turbulence on Near Field Characteristics of Round Jets

**Abstract:** The effect of the small scale turbulence on the development of the round jet is experimentally studied using hot wire anemometry. The small scale turbulence is generated by placing a grid having grid spacing near the nozzle exit. Experiments are carried out for the range of Reynolds numbers (4000, 6000 and 8000). It is observed that the small scale structures present in the jet slows down the jet mixing characteristics and there by retards the decay rate in the near-field region. It is observed that in the grid disturbed jets, the ratio of the turbulent kinetic energy to mean-flow kinetic energy is relatively lower than that of the undisturbed jet without any grid. From the spectral analysis, it is observed that the grid disturbed jets has higher energy content than that of the undisturbed jets.

**Keywords:** grid generated turbulence, hot wire anemometry, jet decay, near-field characteristics, turbulent kinetic energy, spectral analysis

**PACS® (2010).** 47.27.W

\*Corresponding author: **Vasudevan Raghavan:** Department of Mechanical Engineering, Indian Institute of Technology Madras, Chennai 600036, India. E-mail: raghavan@iitm.ac.in

**S. Sivakumar, Ravikiran Sangras:** Department of Mechanical Engineering, Indian Institute of Technology Madras, Chennai 600036, India

## 1 Introduction

Turbulent flow is a very common phenomenon occurring in several applications. Turbulent jets have wide applications in industries. Turbulent jets emerging from nozzles with circular cross-section are commonly called round turbulent jets. Round jet flows are encountered in a variety of engineering applications including chemical processes, combustion, cooling processes, mixing and drying processes. Mixing action between the jet and the surrounding fluid plays an important role in the above-mentioned applications. The characteristics of a turbulent jet flow near to the nozzle region are called near-field characteristics

and form the crucial part of the turbulent jet dynamics. Near-field characteristics of the round jet are mainly dependent on the initial and boundary conditions such as nozzle geometry, flow conditions and fluid properties. The overall aim of the industrial researchers is to optimize the mixing process resulting in both lowest energy consumption and highest mixing rate. Researchers have carried out enormous amount of work in the area of turbulent jets to enhance the jet mixing process.

The structure and development of turbulent jets were studied by Wagnanski and Fiedler [13]. The near-field development and spectra of turbulent jets were reported by Bogusewski and Popiel [1], where it was reported that the near-field region is susceptible to the variations in initial and boundary conditions. Frost and Jambunathan [4] studied the characteristics of the jet evolving from the long pipe and contoured nozzle, and reported that the length of potential core region in the jet evolving from the long pipe is 7% longer than the jet evolving from the contoured nozzle. The effect of different nozzle intrusions on the round jet was studied by Rahai and Wong [10]. Burrattini et al. [2] studied the effect of Reynolds number on the round jet being disturbed by the grids placed at the nozzle exit. They observed that the length of the potential core region in the jet disturbed by the grid is 50% longer than that of the undisturbed jet. Authors observed a significant increase in the turbulent kinetic energy, jet half-width, and reduction in the maximum mean velocity as the result of nozzle intrusion. The effect of nozzle geometry on the turbulent round jet was studied by Quinn [9]. Authors observed higher turbulent intensity in the sharp-edged orifice jet compared to the jet from contoured nozzle, concluded that jet emerging from the sharp-edged orifice has strong mixing characteristics in comparison with the jet issuing from the contoured nozzle. The effect of Reynolds number on the near-field of round jet was studied by Fellouah et al. [3]. They observed reduction in the length of potential core as the Reynolds number was increased.

Researchers have reported adequate amount of work in the near-field of turbulent jets at moderate Reynolds numbers, both in the near and far-field regions. There have been not so many reports in the area of turbulent jets involving disturbances due to the nozzle intrusions. Very

few authors have studied the effect of grid induced turbulence in the jet, especially concentrating on the effect of Reynolds number on the grid induced turbulence on round jets. This paper mainly deals with the small scale disturbances, which are generated from the grids placed near the nozzle exit. These small scale disturbances are controlled by varying the grid spacing.

## 2 Experimental setup

A schematic representation of overall experimental setup is shown in Fig. 1(a). Compressed air at a constant upstream pressure of 750 kPa, and a flow rate of  $0.243 \text{ m}^3/\text{s}$  is supplied from a storage tank of capacity  $20 \text{ m}^3$  through a pressure regulator and rotameter into a settling chamber. A ball valve is used to open or close the circuit securely. The impurities and moisture in the air have been removed by a filter and moisture remover. The settling chamber

consists of honeycomb for straightening the flow and meshes having different spacing (mesh 1 – 1 mm, mesh 2 – 0.5 mm, mesh 3 – 0.25 mm), for eliminating the vortices in the flow. The air stream is subjected to axi-symmetric contraction using a 5th order contracting nozzle, where the contraction ratio is 400:1. The jet emerging from the nozzle exit is ensured to have low turbulent intensity and an almost top-hat profile. Flow domain is in the shape of a square prism with base dimensions of  $0.5 \text{ m} \times 0.5 \text{ m}$  and a height of 0.8 m, surrounded by wire mesh of 1 mm spacing. This wire mesh is optimized for having adequate entrainment with minimum disturbances in the entraining air. Hot-wire probe is accurately positioned at any location in the flow domain by using a three-dimensional manual traverse setup having a swept volume of  $0.5 \text{ m} \times 0.5 \text{ m} \times 0.5 \text{ m}$ .

Meshes (Fig. 1(b)) placed on the nozzle exit section, generates small scale eddies (diameter in the order of  $h$ ) by extracting a part of energy from the mean flow. Meshes with different grid spacing are modelled in CATIA (a com-

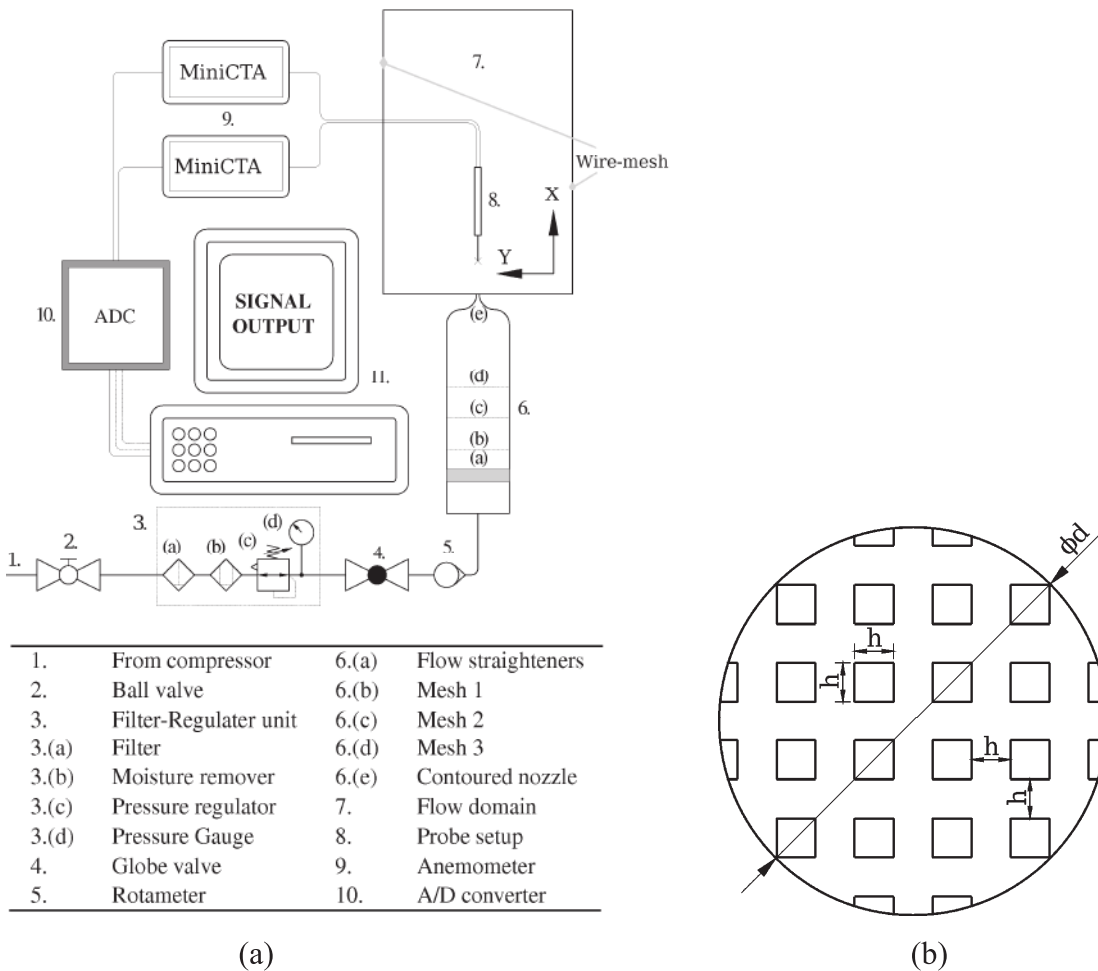


Fig. 1: Schematic view of (a) experimental setup and (b) grid

mercial CAD modelling software), fabricated with the help of Rapid Prototyping machine (Objet Eden 350 V). Nozzle used in the experiment is characterized by two 5th order profiles (similar to bicubic profile), modelled in CATIA and fabricated from the Rapid Prototyping machine.

Stationary hot-wire anemometer, having a wire of  $10\ \mu\text{m}$  diameter and a length of  $1.25\ \text{mm}$ , is used to measure transient velocity data at any location within the jet flow field (component 7 in Fig. 1(a)). It is calibrated using the mean velocity data obtained by a stainless steel Pitot tube having a port diameter of  $0.5\ \text{mm}$ . The mean velocity is calculated from the measured pressure difference, by connecting the Pitot tube to a differential manometer. Olinto and Möller [8] reported about the errors involved in the x-probe hot-wire calibration and presented a relation between the flow velocity, probe angle and the electrical output.

$$E_1^2 - E_0^2 = AU^n \cos^m(\alpha - \delta) \quad (1)$$

$$E_2^2 - E_0^2 = AU^n \cos^m(\alpha + \delta) \quad (2)$$

In equations (1) and (2),  $E_1$  and  $E_2$  are the mean voltage measured on the bridge at a given velocity  $U$ , from wires 1 and 2, respectively. The voltage obtained at zero velocity is designated as  $E_0$ . Further in equations (1) and (2),  $\alpha$  is the angle between the wire and the probe axis,  $\delta$  is the angle between the mean flow direction and the probe axis, and  $A$ ,  $n$ , and  $m$ , are the constants to be determined during calibration.

The hot-wire (component 8 in Fig. 1(a)) loses its heat to the ambient air, primarily due to convection and also due to conduction. This will be proportional to the local flow velocity, which will be sensed by the bridge circuit and amplified by servo amplifier in an instantaneous feedback loop (component 9 in Fig. 1(a)). The analog

output from MiniCTA is converted to digital form using an analog to digital converter (component 10 in Fig. 1(a)) and fed to a computer (component 11 in Fig. 1(a)). The wire temperature is set to  $240^\circ\text{C}$  by setting a corresponding overheat resistance in MiniCTA. As the Reynolds number considered is low ( $4000\text{--}8000$ ), the sampling frequency is set at  $20\ \text{kHz}$ . The number of samples totaling to  $100,000$  are collected maintaining low-pass filtering frequency at  $10\ \text{kHz}$ . Data is acquired from the anemometer with the help of National Instruments DAQ card and is controlled by the commercial software, LabVIEW. The obtained electrical data is converted to velocity data using an in-house code developed in FORTRAN. The post processing of the collected data have been done using Qtiplot and MATLAB.

### 3 Results and discussion

Grids with specific hole-dimensions are placed at the nozzle exit section so as to generate small scale turbulence in the origin of the round jet. The spacing of the grid is in the order of one-tenth of the diameter of the jet, so that eddies generated due to the grids have a diameter in the range of  $1\ \text{mm}$ . The mean kinetic energy of the undisturbed jet is always higher than the jet that is been disturbed by the grid. The reduction in mean kinetic energy is due to the fact that the small scale eddies generated at the nozzle exit extracts a portion of energy from the mean flow. The reduction in the mean flow kinetic energy and the introduction of the small scale eddies considerably affect the near-field development of the round jet. Experiments are carried out by introducing grids having spacing varying from  $0.09d$  to  $0.12d$  (as shown in Fig. 2). Three Reynolds numbers ( $4000$ ,  $6000$  and  $8000$ ) as above are considered.

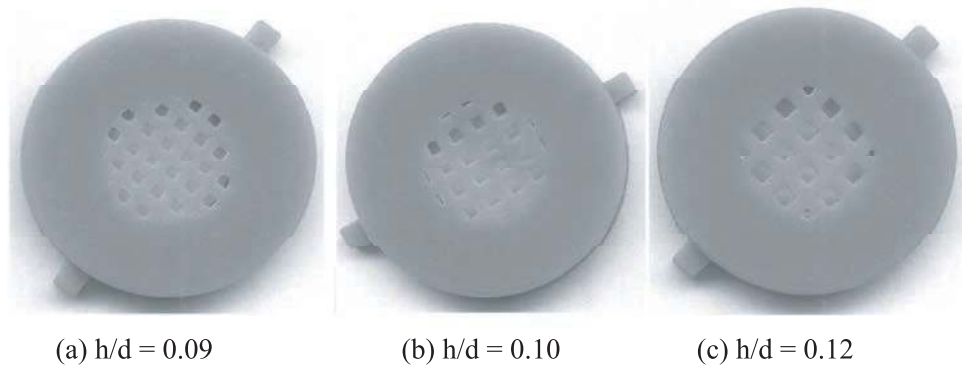


Fig. 2: Photographs of grids used in the experiment

### 3.1 Development of mean velocity

Potential core length is one of the important parameter in characterising the near-field growth of a turbulent jet. The potential core length directly indicates the strength of the initial shear layer around the potential core. Frost and Jambunathan [4] defined the potential core length as “the distance from the nozzle exit to where the axial velocity has decreased to 95% of the initial axial velocity.” In the present study, the same definition is used to calculate the potential core length in the turbulent jet for various Reynolds numbers. Figure 3 show the effect of grid spacing on the potential core length of the round jet for three Reynolds numbers.

In general, the potential core length of the jet issuing through the grid is longer than that of the jet issuing without the grid. This is due to the fact that the disturbed core region of the jet evolving through the grid has higher resistance towards the shearing action of the shearing layer. Also, the variation trend in the potential core length of the undisturbed jet (monotonically decreasing trend) is quite opposite to grid disturbed jets. Among the jets evolving from the grids, the one evolving from the grid having a spacing of 0.10d has the highest potential core length (almost twice of the jet evolving from the undisturbed nozzle) compared to the other cases. Burattini et al. [2] also observed around 50% increase in the length of the potential core for the grid disturbed jet compared to that of the normal round jet. Except for the case of 0.09d grid, the effect of Re is not significant in the case of grid dis-

turbed jets. Taking the case of 0.09d grid, the peculiarity in the case of  $Re = 6000$  is apparent; that is, when Re is increased from 4000 to 6000, the potential core length is seen to increase. With further increase in Re to 8000, there is a reduction in the potential core length. Namer and Ötügen [7] also observed this type of unique behavior with respect to the round jet in the range of Reynolds numbers between 6000 and 7000. They have attributed this to the unique behavior in the initial development of the jet itself.

Decay constant (B) is the quantitative representation of the mean velocity decay rate along axial direction. The constant B and virtual origin  $x_0$  is calculated from equation (3) using mean nozzle exit velocity ( $U_j$ ), mean centreline velocity ( $U_c$ ) and axial distance (x). The decay constant (plotted in Fig. 4) of the jet disturbed by the grids are observed to be higher than those from the undisturbed jet for all the three Reynolds number cases. This decrease in the decay rate for the grid disturbed jets is due the resistance offered by the small scale eddies to the shearing action by the surrounding low momentum fluid. However, the effect of Re is not significant for all the jets emerging through grids. It is also apparent that there is a notable increase in the decay constant when h/d is increased from 0.09 to 0.1; however, there is a notable decrease when h/d of the grid is further increased to 0.12. The increase in the size of the small scale eddies through the grids for h/d = 0.12 case is the reason for its increased decay rate when compared to other grids. This also indicates that there is an optimum grid size that can be used for getting the minimum decay rate.

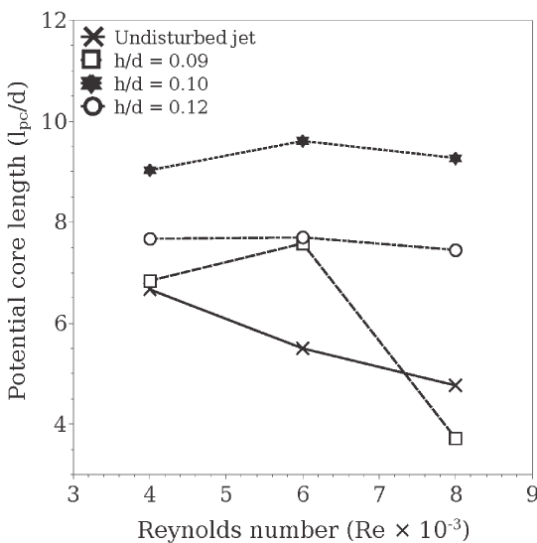


Fig. 3: Variation of potential core length with respect to Reynolds number and grid spacing

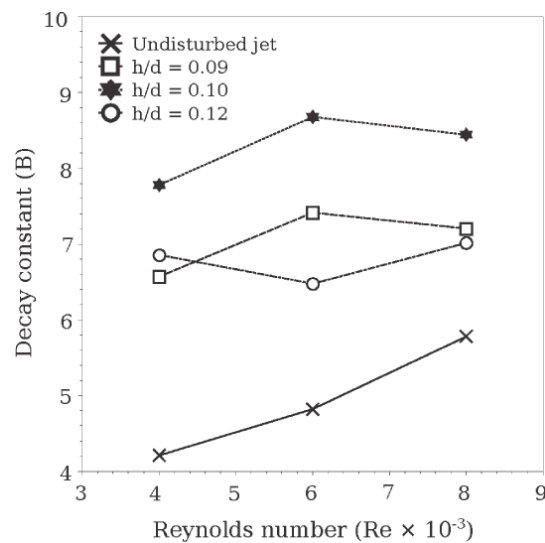


Fig. 4: Variation of decay constant with respect to Reynolds number and grid spacing

$$\frac{U_j}{U_c} = \frac{1}{B} \left( \frac{x}{d} - \frac{x_0}{d} \right) \quad (3)$$

According to the literature the decay constant increases with the increase in the flow Reynolds number. In the present experiments, the undisturbed jet and the jets evolving from grids with different spacing follows the same behaviour except for the Reynolds number of 6000. This effect is seen to be dependent on the grid spacing value as well. As observed in Figs. 3 and 4, these represent a unique nature of Re in the range of 6000 and 7000 (Namer and Ötügen, [7]). Todde et al. [12] have mentioned about the completely different behavior of this range of Re when compared to the behavior at other Reynolds numbers.

It is also observed from Figs. 3 and 4 that the jet disturbed by the grid having a spacing of 0.10d behaves uniquely; it has the highest potential core length and decay constant. This suggests the existence of an optimum grid size and such a jet configuration can be used in applications those demand efficient mixing and distribution of fluids over a large domain without an increase in the Reynolds number.

### 3.2 Effects on the energy distribution of the round jet

The basic analysis of velocity field of the round jet clearly indicates the distinct behaviour of the grid disturbed jet compared to that of the undisturbed jet. Eddies extract a portion of energy from the mean flow and is known as the turbulent kinetic energy. This can be estimated from the fluctuating velocity components in the flow domain. In the present study, a two dimensional turbulent kinetic energy ( $TKE_{2D}$ ) is computed using two fluctuating-velocity components (axial and radial). The circumferential (in the azimuthal direction) fluctuating component of velocity is not included in the calculation, since it is not extracted from the flow domain using cross-wire anemometer.  $TKE_{2D}$  is computed from the fluctuating axial and radial velocities using equation (4) given below.

$$TKE_{2D} = \frac{u_{RMS}^2 + v_{RMS}^2}{2} \quad (4)$$

In equation 4,  $u_{RMS}$  and  $v_{RMS}$  are the root mean square of the fluctuating velocity components along the axial and radial direction, respectively. The turbulent kinetic energy is made non-dimensional by dividing it by the square of the mean centreline velocity measured at the same point.

Figure 5 shows the distribution of turbulent kinetic energy along the centreline of the domain for normal undisturbed jet and for the jets those are disturbed by the grid. It is observed that the rate of generation of TKE is lower for the grid disturbed jets compared to that of the normal jet. Particularly the jet emerging from the grid having a spacing of 0.10d has the lowest rate of generation of turbulent kinetic energy. This is due to the fact that small scale eddies present in the jet decreases the rate of mixing process, therefore, decreasing the conversion rate of mean flow energy to turbulent kinetic energy. Further Fig. 5 shows an increasing trend of non-dimensional TKE for the cases of grid disturbed jets (even at a location of 30d) compared to the normal jets, where TKE sort of plateaus after a particular axial distance depending on Re. This implies that for the grid disturbed jets, the generation of TKE continues also beyond the axial location of 30d from nozzle exit.

The radial spread of the turbulent kinetic energy at an axial location of 15d from the nozzle exit is plotted in Fig. 6. As observed earlier, the energy distribution of the undisturbed jet is quite different for all the Reynolds numbers; the effect of Re is also clearly observed. Turbulent kinetic energy in the undisturbed jet attains maximum value for the Reynolds number of 6000.

This trend is quite clear from the observations of Malmström et al. [6], where it is mentioned that the axial velocity decay or the spread rate did not have a simple relationship with the Reynolds number. As previously discussed, the undisturbed jet has the maximum turbulent kinetic energy compared to the jets evolving from the grids. Even though the undisturbed jet has the maximum turbulent kinetic energy, it diffuses the energy at a faster rate within a radial location of around  $2.5R_{1/2}$ , similar to the jets being disturbed by the grids. This is due to the fact that the small scale eddies present in the grid disturbed jet slows down the diffusion rate of turbulent kinetic energy in the radial direction. From Fig. 6, it is also observed that the distribution of the turbulent kinetic energy across the grid disturbed jet is almost independent of the Reynolds number.

### 3.3 Effects on the homogeneity of the round jet

A jet disturbed by the grids has small scale eddies, which decreases its development rates along the axial and radial directions. This is proved from the comparison of energy distribution of the undisturbed jet with that of the grid disturbed jets. Kejin et al. [5] observed in his experiments

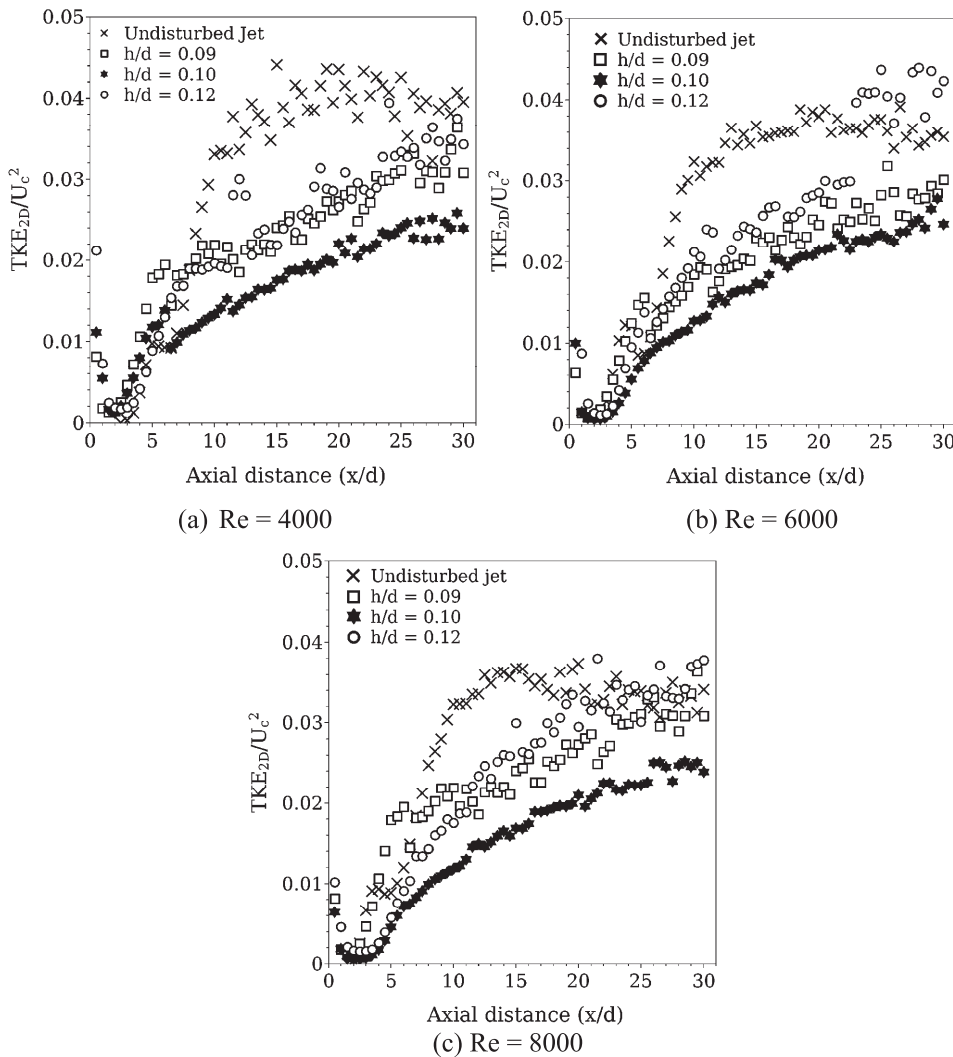


Fig. 5: Two-dimensional turbulent kinetic energy for different nozzle exit conditions

that the small scale eddies will also convert the flow to a homogenous state more effectively than the large scale eddies. Homogenous flow exhibits lesser non-linear behaviour when compared to the normal turbulent flow, and can be identified in the flow domain using many statistical techniques. Kurtosis is selected as one of the statistical quantity to check the homogeneity in the flow. The value of kurtosis increases with the increasing number of peaks in the instantaneous velocity data.

Figure 7 shows the distribution of kurtosis along the jet axis of the round jet. The kurtosis has the value of approximately 3 for normal distribution. The deviations from this value indicate the magnitude of non-linearity present in the flow domain. Energy cascading mechanism consists of continuous transfer of energy from larger eddies to smaller eddies. In Fig. 7, the rise in the kurtosis indicates the energy cascading process, where a portion

of mean flow energy gets converted into turbulent kinetic energy.

In the case of the undisturbed jet, for all the three Reynolds numbers, the energy cascading mechanism starts at an axial location around  $5d$  from the nozzle exit as seen from various parameters before. In the case of the grid disturbed jets, the energy cascading mechanism starts much earlier, at an axial location of  $2d$  from the nozzle exit. This energy cascading mechanism becomes homogenous when eddies involved in the energy cascading process becomes almost identical. The reduction in kurtosis value ( $<3$ ) for the case of undisturbed jet is due to the presence of large scale eddies, which are slow rotating and contributes to the slow variation of the velocity. The increase in the kurtosis value ( $>3$ ) for the undisturbed jet indicates the conversion of large scale eddies to smaller scale eddies. This increase in the kurtosis value in the flow

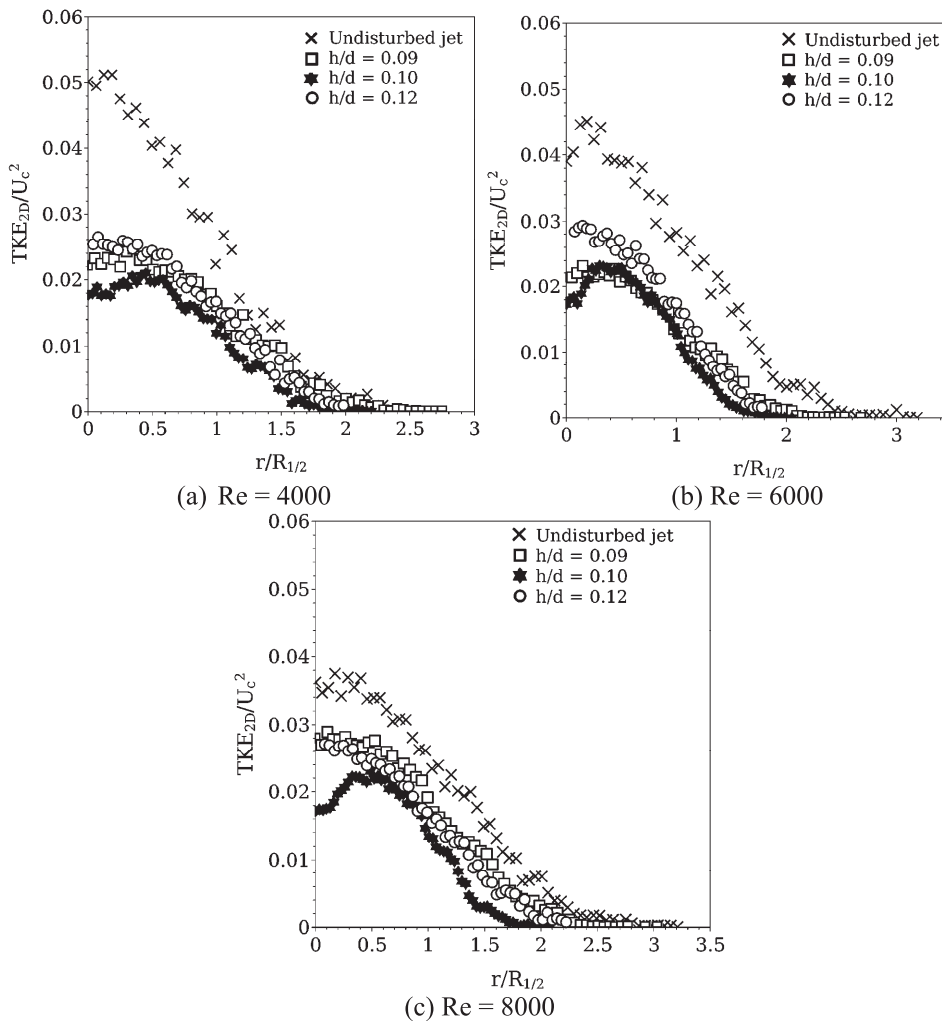


Fig. 6: Radial spread of turbulent kinetic energy for different nozzle exit conditions

domain is also dependent on  $Re$ , ( $x/d = 7$  for  $Re = 4000$ ,  $x/d = 5$  for  $Re = 6000$  and  $x/d = 4$  for  $Re = 8000$ ). The increase in the kurtosis value ( $>3$ ) is due to the presence of relatively large number of small scale eddies. In the case of the jets disturbed by the grids, the energy cascading mechanism becomes homogenous very near to the nozzle exit, at an axial location within  $6d$  itself, irrespective of the Reynolds number. This indicates that the jet disturbed by the grid converts part of its energy into turbulent kinetic energy through the smaller eddies. The span of this non-linear energy cascading mechanism in the cases of undisturbed jets decreases with the increase in the Reynolds number. In the case of the grid disturbed jet, the span of the non-linear energy cascading mechanism is short and almost independent of the Reynolds number.

From Fig. 7, it is clearly observed the kurtosis values peaks at an axial location of around  $4d$  from the nozzle

exit. At this axial location, kurtosis has been analysed along the radial direction for both undisturbed and grid disturbed jets for all the three Reynolds number cases. Figure 8 shows the distribution of kurtosis along the radial direction for all the cases. Sivakumar et al. [11] has mentioned that the undisturbed jet has the intermittency region at a radial location of around  $3R_{1/2}$  from the jet centreline. The intermittency region for the grid disturbed jet is located at a little closer to the centreline when compared to the undisturbed jet, little less than  $3R_{1/2}$ . This is expected from a grid disturbed jet, as its spread rate is lower than that of the undisturbed jet.

The jet which is evolving from the grid with the spacing of  $0.10d$  has the least spread rate among the grid disturbed jets. This case has the intermittency region closer the jet centreline compared to other grid disturbed jets, located at  $2R_{1/2}$ ,  $2.5R_{1/2}$  and  $2R_{1/2}$ , for the Reynolds

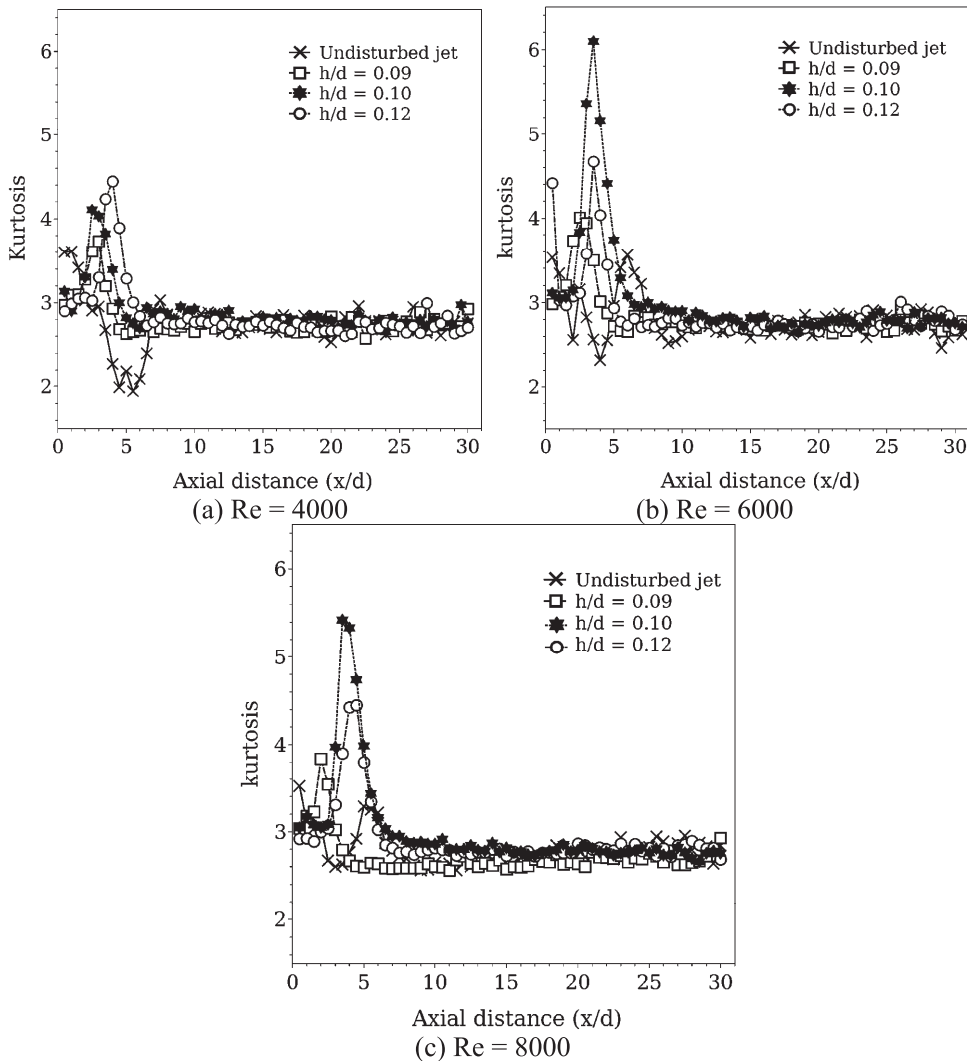


Fig. 7: Axial distribution of kurtosis for jets with different nozzle exit conditions

numbers of 4000, 6000 and 8000, respectively. At the Reynolds number of 6000, the location of the intermittency region is almost the same for all the grid disturbed jets. This indicates that the grid spacing has no effect on the location of intermittency region of the grid disturbed jets at the Reynolds number of 6000.

### 3.4 Effects on the distribution of turbulent eddies in the flow domain

The energy distribution in the fully developed region of a round jet is studied using spectral analysis. FFT analysis has been carried out on the velocity data to obtain the spectral data. The spectral data at a point located on the centreline, at a distance of  $30d$  from the nozzle exit, is compared in Fig. 9 for a jet with Reynolds number of 4000.

At this location, the flow is free from most of the non-linear disturbances that are present at the vicinity of the initial shear layer. This is clearly noted from Fig. 9, as the spectra do not display dominant peaks, as opposed to those shown in the work of Sivakumar et al. [11]. Comparison between various cases in Figs. 9(a)–9(d) shows that the undisturbed jet has lower energy content compared to the grid disturbed jets (area below the spectral curve). Similar trend is observed even in the case of  $Re = 6000$  as shown in Fig. 10. Energy distribution of the undisturbed jet reveals that the large eddies are dominant compared to the small eddies, indicated by the almost zero amplitudes at higher frequencies. In the case of the grid disturbed jets, it is clear that the energy is distributed over a wide range of frequencies. These results indicate that the small scale eddies enhances the long range mixing in the flow domain.

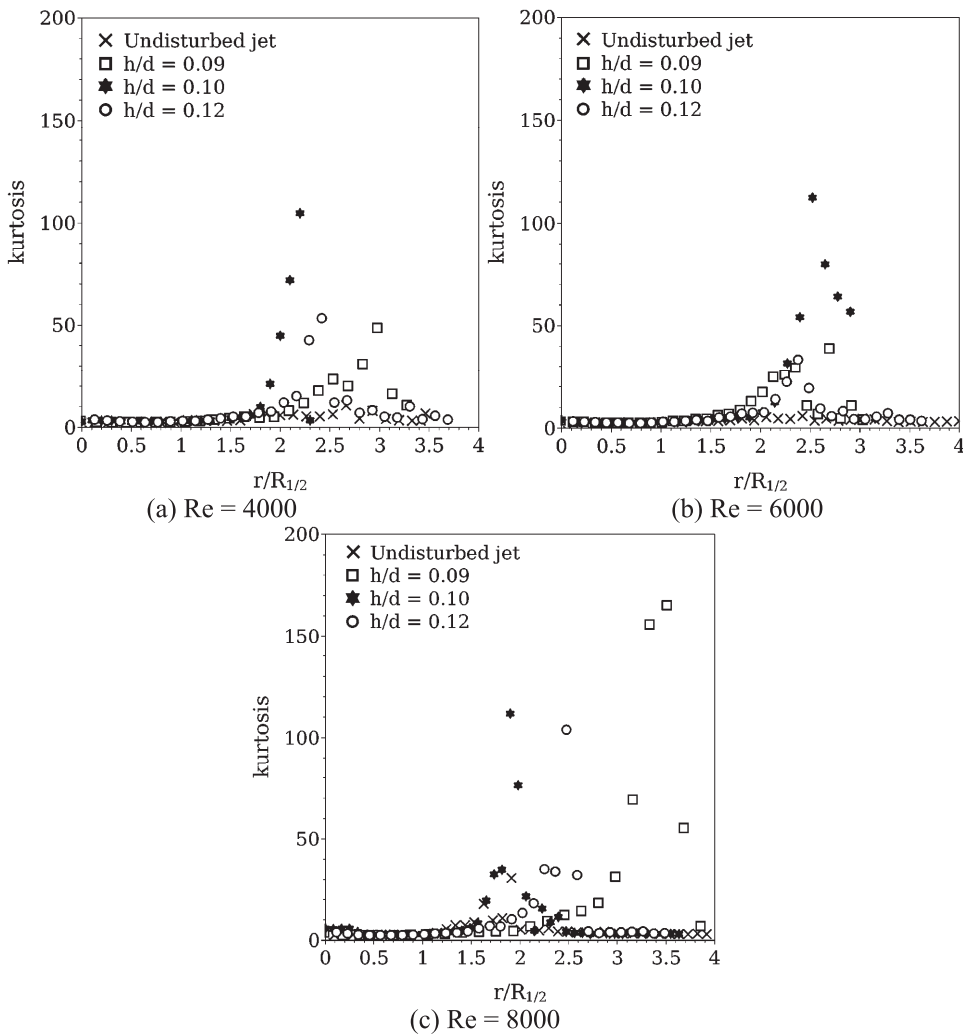


Fig. 8: Radial distribution of kurtosis for jets with different nozzle exit conditions

## 4 Conclusions

The effect of the small scale turbulence (generated by placing grids at the nozzle exit) in the near-field region of a round jet has been studied experimentally using hot wire anemometry. Jet emerging from the grid with the spacing of  $h/d = 0.10$  has largest potential core length among the three grids used. The small scale eddies retards the growth of the round jet along the radial and axial direction in the flow domain. Jet emerging from the grid with the spacing of  $h/d = 0.10$  has the lowest decay rate. Grid disturbed jet has smooth generation of the turbulent kinetic energy compared to the undisturbed normal jet. The location and the span of the transition region are independent of the Reynolds number for the grid disturbed jet. The grid disturbed jet can be effectively used in the applications demanding high Reynolds number flows.

High Reynolds number jets have lower spread and decay rates compared to the lower Reynolds number jets, but require high power. High Reynolds number jets are mainly used in industries in the area of mixing of flow properties through large distances. Grid disturbed jets effectively replace the high Reynolds number jets, thereby reducing the power and resource requirement for the mixing process.

Received: November 17, 2012. Accepted: November 18, 2012.

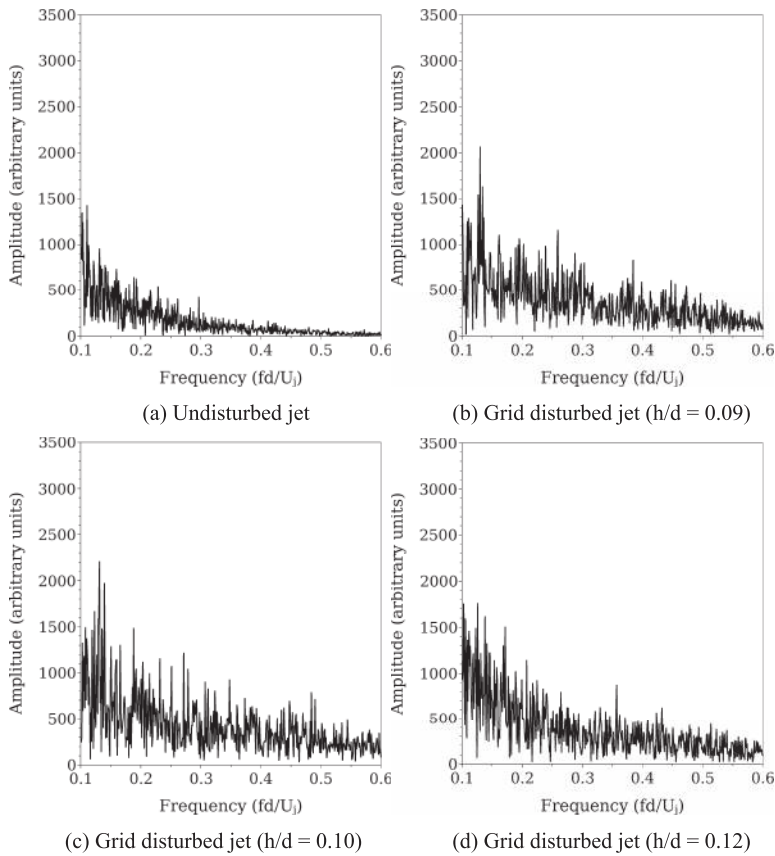


Fig. 9: FFT at an axial location of  $30d$  from nozzle exit, for case of  $Re = 4000$

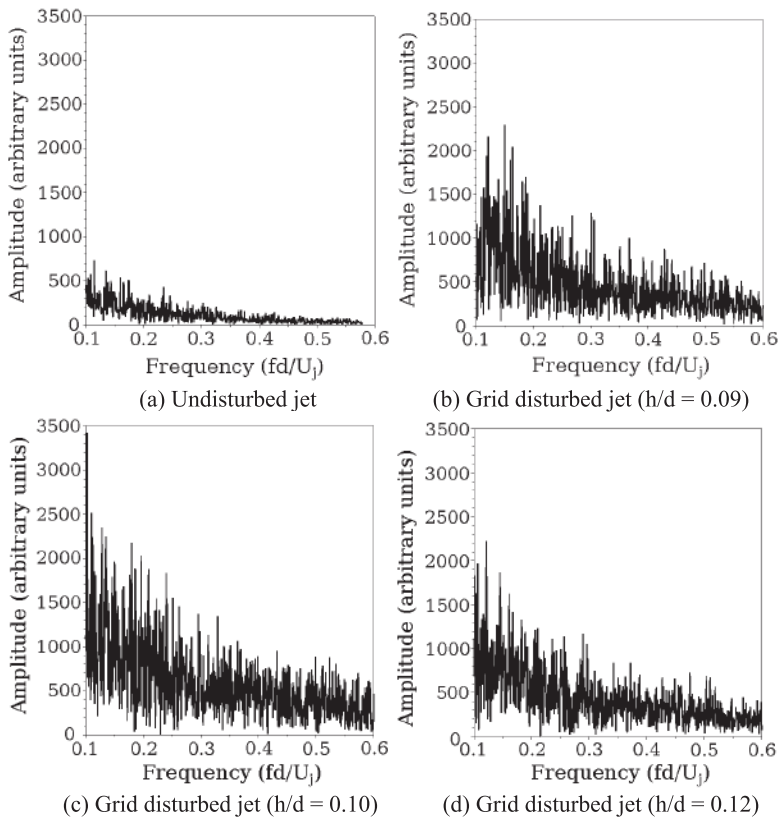


Fig. 10: FFT at an axial location of  $30d$  from nozzle exit, for case of  $Re = 6000$

## References

- [1] L. Bogusewski and C. O. Popiel (1979). Flow structure of the free round turbulent jet in the initial region. *Journal of Fluid Mechanics*, 90, 531–539.
- [2] P. Burattini, R. Antonia, S. Rajagopalan, and M. Stephens (2004). Effect of initial conditions on the near-field development of a round jet. *Experiments in Fluids*, 37, 56–64.
- [3] H. Fellouah, C. Ball, and A. Pollard (2009). Reynolds number effects within the development region of a turbulent round free jet. *International Journal of Heat and Mass Transfer*, 52, 3943–3954.
- [4] S. Frost and K. Jambunathan (1996). Effect of nozzle geometry and semi-confinement on the potential core of a turbulent axisymmetric free jet. *Int. Comm. Heat Mass Transfer*, 23, 155–162.
- [5] M. Kejin, W. Yue, Z. Zhedean, and N. Chaoqun (2007). Modification of premixed combustion in shear layers by grid turbulence. *Frontiers of Energy and Power Engineering in China*, 1(2), 245–250.
- [6] T.G. Malmström, A.T. Kirkpatrick, B. Christensen, and K.D. Knappmiller (1997). Centreline velocity decay measurements in low-velocity axisymmetric jets. *Journal of Fluid Mechanics*, 346(1), 363–377.
- [7] I. Namer and M.V. Ötügen (1988). Velocity measurements in a plane turbulent air jet at moderate Reynolds numbers. *Experiments in Fluids*, 6(6), 387–399.
- [8] C. Olinto and S. Möller (2004). X-probe calibration using Collis and William's equation. In *10th Brazilian Congress of Thermal Sciences and Engineering*.
- [9] W. Quinn (2006). Upstream nozzle shaping effects on near field flow in round turbulent free jets. *European Journal of Mechanics B/Fluids*, 25, 279–301.
- [10] H. Rahai and T. Wong (2002). Velocity field characteristics of turbulent jets from round tubes with coil inserts. *Applied Thermal Engineering*, 22, 1037–1045.
- [11] S. Sivakumar, S. Ravikiran, and V. Raghavan (2012). Characteristics of turbulent round jets in its potential-core region. *International Journal of Mechanical and Aerospace Engineering*, 6, 119–125.
- [12] V. Todde, P.G. Spazzini, and M. Sandberg (2009). Experimental analysis of low-Reynolds number free jets. *Experiments in Fluids*, 47, 279–294.
- [13] I. Wagnanski and H. Fiedler (1969). Some measurements in the self-preserving jet. *Journal of Fluid Mechanics*, 38, 577–612.

